PSD-95 is required for activity-driven synapse stabilization

Ingrid Ehrlich*, Matthew Klein, Simon Rumpel†, and Roberto Malinow

Cold Spring Harbor Laboratory, Cold Spring Harbor, NY 11724

Communicated by Richard L. Huganir, Johns Hopkins University School of Medicine, Baltimore, MD, December 14, 2006 (received for review May 15, 2006)

The activity-dependent regulation of α-amino-3-hydroxy-5-methyl-4-isoxazolepropionic acid (AMPA)-type glutamate receptors and the stabilization of synapses are critical to synaptic development and plasticity. One candidate molecule implicated in maturation, synaptic strengthening, and plasticity is PSD-95. Here we find that acute knockdown of PSD-95 in brain slice cultures by RNAi arrests the normal development of synaptic structure and function that is driven by spontaneous activity. Surprisingly, PSD-95 is not necessary for the induction and early expression of long-term potentiation (LTP). However, knockdown of PSD-95 leads to smaller increases in spine size after chemically induced LTP. Furthermore, although at this age spine turnover is normally low and LTP produces a transient increase, in cells with reduced PSD-95 spine turnover is high and remains increased after LTP. Taken together, our data support a model in which appropriate levels of PSD-95 are required for activity-dependent synapse stabilization after initial phases of synaptic potentiation.

AMPA receptor | long-term depression | long-term potentiation | postsynaptic density

Modifications in synaptic strength and stabilization of synapses underlie developmental and activity-dependent plasticity in the brain. Understanding their molecular mechanisms provides insight into behavioral plasticity and brain dysfunction during disease. One postsynaptic modification regulating synaptic strength is the delivery and removal of α-amino-3-hydroxy-5-methyl-4-isoxazolepropionic acid (AMPA)-type glutamate receptors (1–4). Recently, PSD-95, a member of the MAGUK (membrane-associated guanylate kinase) family, has been suggested to play important roles in synaptic plasticity in hippocampus and cortex by regulating AMPA-R trafficking. These studies used overexpression of wild-type and mutant forms of PSD-95 and suggested that PSD-95 drives synaptic maturation, controls AMPA-R number at synapses, and participates in receptor delivery or stabilization during synaptic plasticity *in vitro* and *in vivo* (5–9). Moreover, stronger synapses with increased PSD-95 levels show enhanced synaptic depression [long-term depression (LTD)] (7, 8). Because MAGUKs are highly homologous and several of them are present at hippocampal synapses (10, 11), issues of specificity weaken the conclusions of such studies. Predictions from overexpression experiments are that loss of PSD-95 should affect basal synaptic properties and strength as well as bidirectional synaptic plasticity. However, a genetic approach using mice modified at the PSD-95 locus showed enhanced long-term potentiation (LTP) and impaired learning (12) but no change in basal synaptic function, which might be due to undetected compensatory mechanisms. Here we examined the function of endogenous PSD-95 by a temporally and spatially restricted knockdown approach using RNAi.

We find that knockdown of PSD-95 arrests the functional and morphological development of glutamatergic synapses. Although induction and early LTP are largely unaffected, spine morphological changes are reduced and spines are less stable over longer time periods. Our results suggest that PSD-95 is required for receptor and synapse stabilization during development and after activity-driven synaptic potentiation.

Results

We designed short hairpin RNAs (shRNAs) that knocked down recombinant PSD-95 in heterologous cells (data not shown) and confirmed their efficacy against endogenous PSD-95 in neurons. After global transfection in hippocampal cultures, effective (Hp1 and Hp2), but not a control (Scr1), shRNA reduced PSD-95 expression in Western blots [supporting information (SI) Fig. 8 *a* and *b*]. Using sparse transfection, effective shRNA also reduced PSD-95 immunoreactivity in somata and dendrites of transfected vs. neighboring control neurons in culture (SI Fig. 8 *c* and *d*). Importantly, expression of Hp1 for 2–3 days in slice cultures also reduced PSD-95 immunoreactivity in individual spines of CA1 neurons. Compared with GFP-expressing neurons, the fraction of spines with undetectable levels of PSD-95 increased ≈2-fold, and in spines with immunoreactivity, levels decreased ≈2- to 3-fold (SI Fig. 9). We also validated this method by confirming that overexpression increased PSD-95 immunoreactivity in all spines (SI Fig. 9). Although the morphology of shRNA-transfected neurons appeared normal, we were concerned about off-target effects (13) or interference with miRNA pathways (14) that could perturb gross morphology and membrane properties. This is unlikely, because two measures of these effects, input resistance and membrane capacitance, were not altered by shRNA expression (SI Fig. 10). Last, because PSD-95 can interact with K^+ channels (10), knockdown could affect passive and active membrane properties. However, current-clamp measurements of membrane potential, input resistance, and spiking behavior show no significantly changes (SI Fig. 11). In summary, our shRNAs have no adverse effects on morphology or passive and active electrical properties of neurons that would compromise data interpretation.

Knockdown of PSD-95 Decreases Synaptic Strength. If PSD-95 participates in synaptic maturation and regulation of synaptic strength, acute knockdown should decrease synaptic transmission. To prevent effects on early synaptogenesis and network activity, we perturbed PSD-95 in a few neurons per slice, and after initial synaptic connectivity in the hippocampus has been established (15, 16). Consistent with our hypothesis, and complementary to findings that overexpression increases synaptic strength (6, 7, 9), acute knockdown of PSD-95 by Hp1 led to a decrease in AMPA-mediated excitatory postsynaptic currents (EPSCs) in CA1 neurons (Fig. 1 *a* and *d*). This decrease in

Author contributions: I.E. and R.M. designed research; I.E., M.K., and S.R. performed research; I.E. and S.R. analyzed data; and I.E. and R.M. wrote the paper.

The authors declare no conflict of interest.

Abbreviations: EPSC, excitatory postsynaptic current; mEPSC, miniature EPSC; AMPA, α-amino-3-hydroxy-5-methyl-4-isoxazolepropionic acid; LTP, long-term potentiation; LTD, long-term depression; shRNA, short hairpin RNA; Div, days *in vitro*; TOR, turnover rate; APV, 2-amino-5-phosphonovaleric acid.

*To whom correspondence should be sent at the present address: Friedrich Miescher Institute, Maulbeerstrasse 66, 4058 Basel, Switzerland. E-mail: ingrid.ehrlich@fmi.ch.

†Present address: Research Institute of Molecular Pathology, Dr. Bohr-Gasse, A-1030 Vienna, Austria.

This article contains supporting information online at www.pnas.org/cgi/content/full/0609307104/DC1.

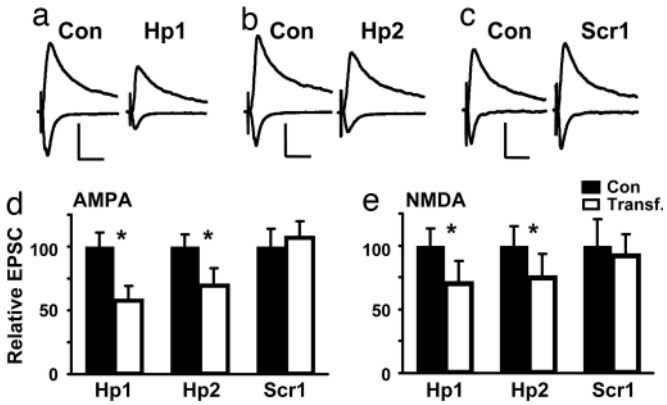

Fig. 1. Knockdown of PSD-95 decreases synaptic strength. (*a–c*) EPSCs recorded from pairs of CA1 pyramidal neurons at −60 or +40 mV (one control and one expressing shRNA). (*a* and *b*) Hp1 and Hp2 decreased AMPA-EPSCs and, to a lesser extent, NMDA-EPSCs. (*c*) Scr1 had no effect on transmission. (Scale bars: 50 pA and 40 ms.) (*d*) For Hp1 and Hp2, AMPA-EPSCs decreased to 57.9 ± 11.4% ($n = 22$, $P < 0.001$) and to 70.2 ± 9.4% of control ($n = 12$, $P < 0.05$); there was no change for Scr1 (107.6 ± 14.0%, $n = 14$, $P = 0.83$). (*e*) For Hp1 and Hp2, NMDA-EPSCs decreased to 71.1 ± 13.3% ($n = 24$, $P = 0.02$) and to 75.6 ± 15.1% of control ($n = 11$, $P = 0.01$); there was no change for Scr1 (92.3 ± 20.2%, $n = 14$, $P = 0.68$).

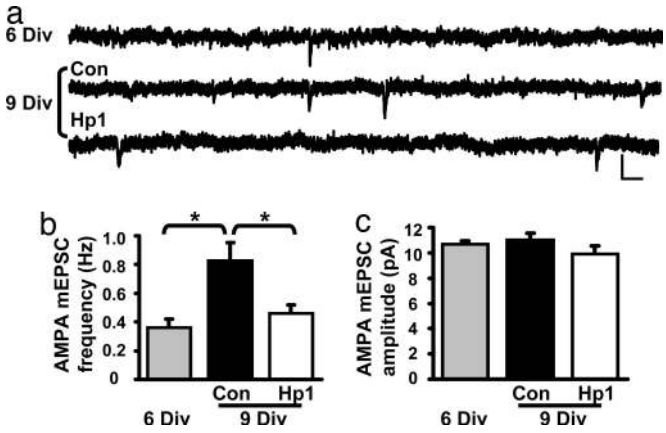

Fig. 2. Knockdown of PSD-95 prevents the developmental increase in synapses with functional AMPA-Rs. (*a*) AMPA-mEPSCs recorded at −60 mV from CA1 neurons at 6 Div and 9 Div (one control and one expressing Hp1 for 3 days). (Scale bars: 20 pA and 50 ms.) (*b*) The increase in mEPSC frequency from 0.36 ± 0.06 Hz ($n = 13$) to 0.83 ± 0.12 Hz ($n = 11$) ($P < 0.001$) was prevented by Hp1 (0.46 ± 0.06 Hz, $n = 11$, $P = 0.01$ vs. 9 Div). (*c*) There was no difference in average mEPSC amplitude in a cell-wise comparison (6 Div: 10.7 ± 0.2 pA, $n = 13$; 9 Div Con: 11.0 ± 0.5 pA, $n = 11$; 9 Div Hp1: 9.9 ± 0.6 pA, $n = 11$; $P > 0.15$).

AMPA-EPSCs was accompanied by a smaller decrease in the late EPSC component at +40 mV, mediated by NMDA-Rs (Fig. 1 *a* and *e*). Importantly, a second shRNA (Hp2) directed against PSD-95 had the same effect, whereas a control shRNA (Scr1) did not effect synaptic transmission (Fig. 1 *b–e*). To investigate whether a subunit switch underlay or accompanied the apparent change in NMDA currents, we recorded pharmacologically isolated NMDA-EPSCs. Both the peak amplitude and the late component decreased similarly (SI Fig. 12*a*). Decay kinetics and susceptibility to the NR2B subunit-specific antagonist Ifenprodil were not altered (SI Fig. 12 *b* and *c*), suggesting no detectible change in properties of synaptic NMDA-Rs over 3 days. To characterize the relationship between changes in AMPA-EPSCs and NMDA-EPSCs and time course of synaptic depression, we recorded 2–7 days after PSD-95 knockdown. Initially, the decrease in AMPA-EPSCs was significantly larger than for NMDA-EPSCs and associated with a lower AMPA/NMDA ratio. Later, AMPA-EPSCs and NMDA-EPSCs were similarly altered with no change in AMPA/NMDA ratio (SI Fig. 13 *a* and *b*). Our hypothesis is that initial changes in strength of AMPA-EPSCs are followed by changes in NMDA-EPSCs and, consequently, readjustment of AMPA/NMDA ratios (17–19). Thus, we subsequently focused on effects of early knockdown (2–3 days).

Knockdown of PSD-95 Prevents the Developmental Increase in Synapses with Functional AMPA-Rs. Excitatory synapses in the hippocampus undergo activity-dependent changes within several days *in vivo* or *in vitro*, among them increases in AMPA/NMDA ratio of evoked transmission and in frequency of AMPA miniature EPSCs (mEPSCs) (16, 17, 19). Together with immunolabeling results (20), this suggested an increase in synapses containing functional AMPA-Rs. One possibility is that knockdown of PSD-95 prevents the developmental increase in functional synapse number. Alternatively, the number of synapses could increase, but the amount of functional receptors could be reduced by other mechanisms, or a combination of decrease in synapse and receptor number. To distinguish between these possibilities, we compared amplitudes and frequencies of AMPA-mEPSCs. We detected an increase in mEPSC frequency between 6 and 7 days *in vitro* (Div) and 9 and 10 Div, which was absent in neurons with knockdown of PSD-95 for 3 days (Fig. 2 *a* and *b*). There was no detectable change in mEPSC amplitude (Fig. 2*c*). Thus, our results support the hypothesis that loss of PSD-95 prevents the developmental increase in the number of synapses expressing functional AMPA-Rs.

Knockdown of PSD-95 Prevents Developmental Changes in Spine Density and Morphology. Concomitant with changes in synaptic strength, activity drives spine morphological changes during development and plasticity; e.g., large mushroom spines become more prominent and may be associated with mature synapses of high strength (16, 21–23). We wondered whether knockdown of PSD-95 also perturbed changes in spine morphology. We imaged spines at 7 Div and determined how they changed when neurons expressed control (Scr1) or effective shRNA (Hp1) for 3 days (Fig. 3*a*). Between 7 and 10 Div, we found a significant increase in spine density and spine size that was absent when PSD-95 was knocked down (Fig. 3 *b* and *d*). In addition and consistent with previous findings (16, 23), stubby spines became less, and mushroom spines became more frequent, a process that was also prevented by PSD-95 knockdown (Fig. 3*c*). Interestingly, cumulative distributions show a uniform shift (except for very large spines which were rare but present in all groups), indicating that the entire population shifted, rather than a selective change in a subpopulation of spines. Our findings that knockdown of PSD-95 not only prevented increases in synaptic strength but also changes in spine density and morphology, suggest that synapses may be arrested in a more immature state. Corresponding changes in spine density and mEPSC frequency are consistent with a reduction in functional synapse number.

Activity Blockade Occludes the Decrease in Glutamatergic Function by Knockdown of PSD-95. Because knockdown of PSD-95 appears to arrest processes at glutamatergic synapses that are normally driven by spontaneous activity and NMDA-R activation (17, 19), one prediction is that activity blockade should occlude the effects of knockdown of PSD-95. To test this directly, we knocked down PSD-95 in slices maintained in drugs that block neuronal activity. If occlusion occurs, evoked EPSCs should not differ between control and nearby knockdown neurons. Indeed, we found that block of spontaneous activity by high Mg^{2+} or TTX occluded both the decrease synaptic strength of AMPA-EPSCs and NMDA-

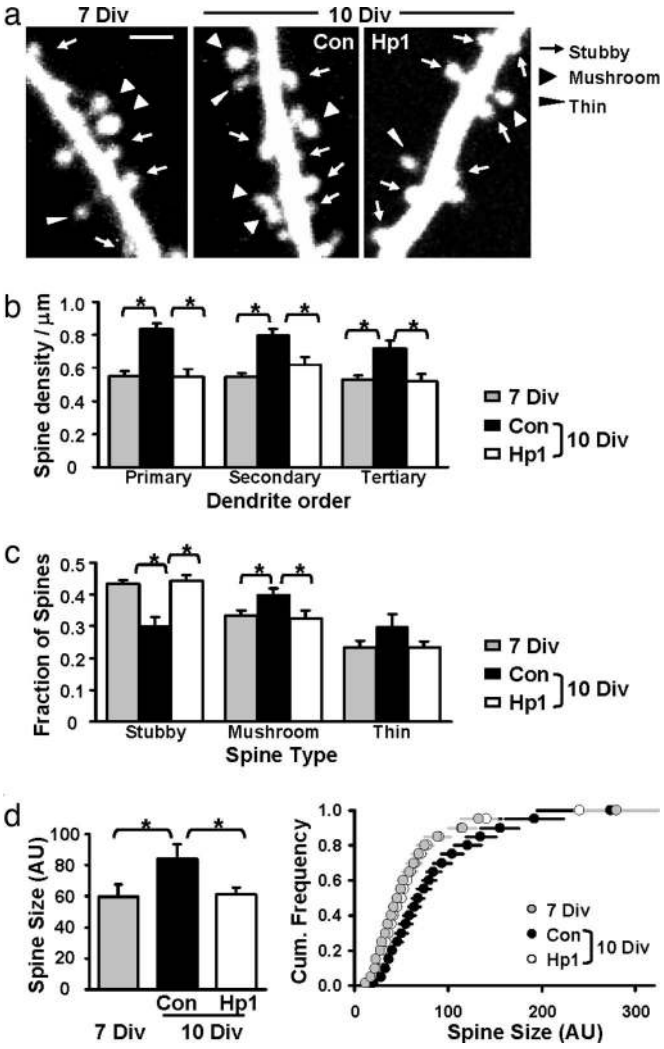

Fig. 3. Knockdown of PSD-95 arrests spine morphological development. (*a*) Two-photon images of secondary apical dendrites at 7 Div, and at 10 Div after expressing control or effective shRNA for 3 days. (Scale bar: 2 μm.) (*b*) Hp1 prevented the increase in spine density (*, $P < 0.01$). Primary dendrites: 0.55 ± 0.03 (7 Div), 0.84 ± 0.04, and 0.54 ± 0.05 spines per micrometer (Con and Hp1 at 10 Div). Secondary dendrites: 0.55 ± 0.02 (7 Div), 0.84 ± 0.04, and 0.62 ± 0.05 spines per micrometer (Con and Hp1 at 10 Div). Tertiary dendrites: 0.53 ± 0.02 (7 Div), 0.72 ± 0.05, and 0.52 ± 0.04 spines per micrometer (Con and Hp1 at 10 Div). No difference was observed between 7 Div and Hp1 at 10 Div ($P > 0.13$). (*c*) Hp1 prevented changes in spine type (*, $P < 0.05$). Fraction of stubby spines: 0.43 ± 0.01 (7 Div), 0.30 ± 0.03, and 0.44 ± 0.02 (Con and Hp1 at 10 Div). Fraction of mushroom spines: 0.33 ± 0.02 (7 Div), 0.40 ± 0.02, and 0.32 ± 0.03 (Con and Hp1 at 10 Div). The fraction of thin spines did not change ($P > 0.16$). (*d*) Hp1 prevented spine size changes (*, $P < 0.04$). Average spine sizes were 59.8 ± 7.9 (7 Div), 84.1 ± 9.7 (Con 10 Div), and 61.1 ± 4.7 (Hp1 10 Div; $P = 0.44$ vs. 7 Div) in arbitrary units (AU). (*Right*) Cumulative distributions of spine sizes. $n = 6$ cells per group.

EPSCs (Fig. 4 *a*, *b*, *d*, and *e*). Consistent with a role for NMDA-R signaling, 2-amino-5-phosphonovaleric acid (APV) also occluded the decrease of AMPA-EPSCs (Fig. 4 *c* and *d*). Interestingly, NMDA-EPSCs were still decreased (Fig. 4*e*), which may indicate different requirements for the maintenance of NMDA-Rs or silent synapses, containing NMDA-Rs only. Taken together, our results lend support to the idea that PSD-95 participates in activity-driven increases in glutamatergic function.

Normal Levels of PSD-95 Are Not Required for Induction and Early Expression of LTP. Synaptic strengthening by spontaneous activity and LTP share some similar mechanisms (19, 24, 25). Previous

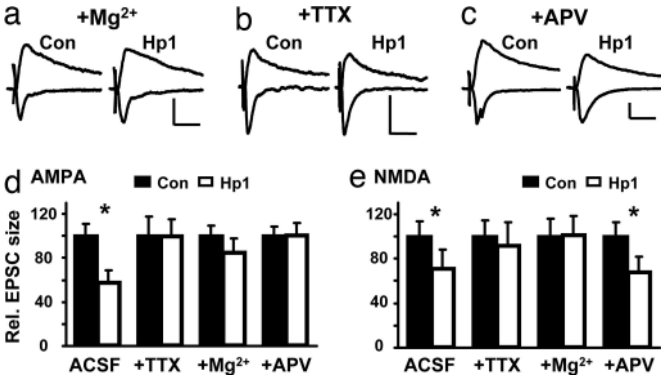

Fig. 4. Decrease in synaptic strength by knockdown of PSD-95 is occluded by activity blockade. (*a–c*) EPSCs recorded from pairs of CA1 neurons at −60 or +40 mV after incubation in high Mg^{2+}, TTX, or APV for 2–3 days showed no change, except for NMDA-EPSCs after incubation in APV. (Scale bars: 20 pA and 40 ms.) (*d*) In Hp1-expressing neurons, AMPA-EPSCs were 99.8 ± 15.3% (34.1 ± 6.0 vs. 34.0 ± 5.2 pA, $n = 13$, $P = 0.98$) for TTX-treated neurons, 85.0 ± 12.7% (34.7 ± 3.1 vs. 29.5 ± 3.8 pA, $n = 17$, $P = 0.23$) for Mg^{2+}-treated neurons, and 100.7 ± 10.9% of control (27.2 ± 2.2 vs. 27.4 ± 3.0 pA, $n = 12$, $P = 0.96$) for APV-treated neurons. (*e*) In Hp1-expressing neurons, NMDA-EPSCs were 91.6 ± 21.1% (18.3 ± 2.5 vs. 16.7 ± 3.5 pA, $n = 12$, $P = 0.38$) for TTX-treated neurons, 101.5 ± 16.7% (17.7 ± 2.8 vs. 18.0 ± 3.0 pA, $n = 12$, $P = 0.93$) for Mg^{2+}-treated neurons, and 68.2 ± 13.6% of control (15.1 ± 1.9 vs. 10.2 ± 1.5 pA, $n = 10$, $P = 0.02$) for APV-treated neurons.

studies have suggested that PSD-95 participates in LTP (8, 9). We thus examined functional changes after pairing-induced LTP in control (nontransfected or Scr1-expressing) and Hp1-expressing neurons. In another set of experiments, we prevented the decrease in NMDA-EPSCs by preincubating slice cultures in TTX (*cf.* Fig. 4). Surprisingly, in all conditions, time course and relative levels of LTP were not significantly altered 35 min after pairing (Fig. 5 *a*, *b*, and *e*). Postsynaptic signaling mediating LTP switches from being PKA- to being CaMKII-dependent, a developmental process that is normally completed in the second postnatal week, i.e., before we perform our experiments (24–26). We explored the possibility that LTP in PSD-95 knockdown cells uses more "immature" signaling mechanisms. However, we find that blocking CaMKII-activity prevented induction and expression of LTP in both groups (Fig. 5 *c–e*). We conclude that normal PSD-95 levels are not required for CaMKII-dependent induction and expression of functional changes during the first 35 min of LTP.

Knockdown of PSD-95 Affects Spine Morphological Changes After cLTP. Because reducing PSD-95 levels arrested spine morphological changes over the course of days, we wondered whether it also affects activity-driven changes on a shorter timescale. We induced global potentiation of synapses using a chemical LTP protocol (cLTP) that shares properties with electrically evoked LTP (22, 27) and followed modifications of spines by two-photon imaging. We used older cultures in these experiments (see methods), after confirming that Hp1 was still effective at reducing PSD-95 levels (SI Fig. 9) and synaptic strength (SI Fig. 13 *c* and *d*). Consistent with previous results, we find that in control neurons, spines present during the entire imaging session increased their volume on average by ≈50% (22). In neurons expressing Hp1 for 3 days, the increase in spine size was significantly reduced (Fig. 5 *f* and *g*).

Interestingly, several other observations in these experiments suggested that spines were less stable after PSD-95 knockdown. In control neurons, almost all spines observed during baseline persisted for the entire imaging session (98 ± 1.0%, $n = 4$ cells, 312 spines), whereas in Hp-expressing neurons this fraction was

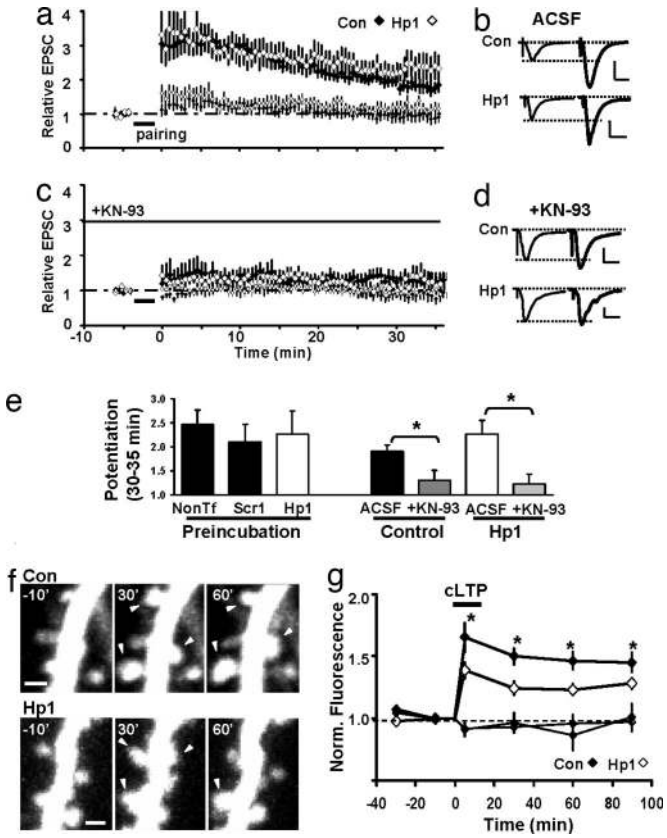

Fig. 5. Knockdown of PSD-95 affects morphological but not early functional changes during LTP. (*a–e*) Normal levels of PSD-95 are not required for induction and early expression of LTP. (*a*) No difference in LTP between control (nontransfected, $n = 10$) and Hp1-expressing ($n = 8$) ($P = 0.23$) neurons. (*c*) LTP in control and Hp1-expressing neurons was sensitive to the CaMKII blocker KN-93 applied 20 min before and during induction. (*b* and *d*) Average EPSCs before and 30–35 min after pairing. (Scale bars: 20 pA and 20 ms.) (*e*) Summary of all LTP data: When preincubation in TTX was used to prevent decrease in NMDA-EPSCs, no difference in LTP was observed (nontransfected: 2.46 ± 0.31, $n = 7$; Scr1: 2.10 ± 0.37, $n = 7$; Hp1: 2.27 ± 0.48, $n = 8$; $P > 0.46$). Under normal conditions, LTP was 1.9 ± 0.14 ($n = 10$) in control neurons and blocked by KN-93 (1.31 ± 0.21, $n = 9$, $P < 0.03$). In Hp1 neurons, LTP was 2.26 ± 0.28 ($n = 8$) and blocked by KN-93 (1.23 ± 0.21, $n = 7$, $P < 0.02$). (*f* and *g*) Knockdown of PSD-95 affects spine size changes after cLTP. (*f*) Spine changes (arrowheads) after cLTP in a control and a Hp1-neuron. (Scale bars: 1 μm.) (*g*) cLTP led to smaller increases in spine volume in Hp1 (26 ± 4%, $n = 3$ cells, 216 spines) than in control neurons (46 ± 7%, $n = 3$ cells, 171 spines) ($P < 0.04$).

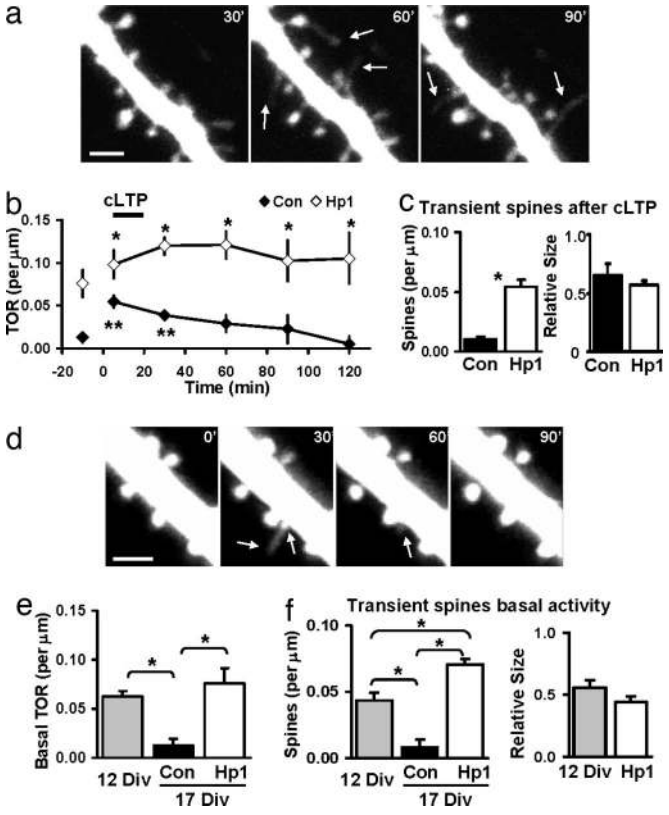

Fig. 6. Knockdown of PSD-95 increases spine turnover and transient spines. (*a*) Dendrite of Hp1 neuron imaged 30–90 min after cLTP showing extension and retraction of protrusions (arrows). (Scale bar: 2 μm.) (*b*) Spine TOR before and after cLTP increased in Hp1 vs. control neurons (*, $P < 0.04$; $n = 4$ cells). In control neurons, TOR increased transiently after cLTP (**, $P < 0.05$). (*c*) Fraction of transient spines (lifetime < 1 h) after cLTP was increased in Hp1 vs. control neurons (0.010 ± 0.002 vs. 0.054 ± 0.006 spines per micrometer per 30 min, $n = 4$ cells, $P < 0.01$). Transient spines were smaller (normalized to mean stable spine size; Con: 0.65 ± 0.10, $n = 25$; Hp1: 0.57 ± 0.04, $n = 69$). (*d*) Dendrite of a control neuron (12 Div) showing transient protrusions (arrows). (Scale bar: 2 μm.) (*e*) Basal TOR decreased over development and remained high after knockdown (12 Div: 0.063 ± 0.006, $n = 3$; 17 Div Con: 0.013 ± 0.007, $n = 5$; 17 Div Hp1: 0.076 ± 0.016 spines per micrometer per 30 min, $n = 4$ cells; *, $P < 0.006$). (*f*) The fraction of transient spines decreased but was elevated in Hp1 vs. control neurons (12 Div: 0.043 ± 0.006, $n = 3$; 17 Div Con: 0.008 ± 0.006, $n = 5$; 17 Div Hp1: 0.071 ± 0.004 spines per micrometer per 30 min, $n = 4$ cells; *, $P < 0.012$). Transient spines were smaller (12 Div: 0.55 ± 0.06, $n = 29$; Hp1: 0.44 ± 0.05, $n = 25$).

significantly reduced (85 ± 0.5%, $n = 4$ cells, 327 spines) ($P < 0.001$). After cLTP, there was a larger fraction of transient spines (lifetime < 1 h) in knockdown vs. control neurons, and transient spines were smaller than stable spines (Fig. 6 *a* and *c*). Last, the number of spine additions and losses, the turnover rate (TOR), was significantly increased after knockdown of PSD-95, both before and after cLTP (Fig. 6*b*). In knockdown neurons, the high TOR was due to approximately equal contribution of spine addition and loss and resulted in little change in absolute spine number. In control neurons, the TOR increased transiently after cLTP (Fig. 6*b*), reflecting mostly addition of spines. In summary, knockdown of PSD-95 resulted in decreased spine size changes and a larger number of transient spines after cLTP, suggesting that stabilization of spine morphological changes may be impaired.

Increased Spine Turnover After Knockdown of PSD-95 Resembles That in Younger Neurons. Next we explored the possibility that spines in PSD-95 knockdown neurons were also less stable during spontaneous activity. This may reflect behavior of spines in younger neurons, where transient and motile protrusions are prominent, and probe the neuropil for synaptic partners (28). We determined TOR and fraction of transient spines during basal activity in neurons age-matched to cLTP experiments (14 Div plus 3 days with or without knockdown of PSD-95) during basal activity, and compared those groups to younger neurons (Div12). We found that both transient spines and spine TOR decreased with development (Fig. 6 *d–f*). When PSD-95 was knocked down, the TOR remained elevated at levels observed in young neurons, but the fraction of transient spines was even larger (Fig. 6 *e* and *f*). These small transient spines resembled motile protrusions not associated with PSD-95 clusters (29, 30). Our results suggest that knockdown of PSD-95 not only impaired spine changes after cLTP, but also decreased spine stability during spontaneous activity, which could underlie the observed arrest of synaptic stabilization and maturation.

Knockdown of PSD-95 Impairs LTD. Synapses are bidirectionally regulated by activity and may have certain requirements for

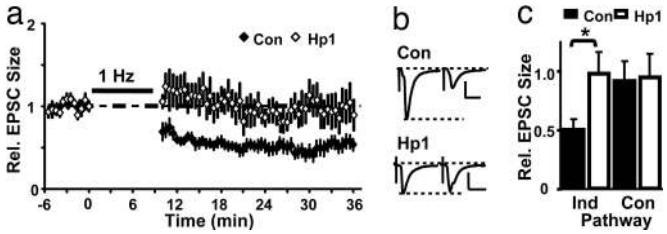

Fig. 7. Knockdown of PSD-95 impairs LTD. (*a*) Synaptic depression after pairing-induced LTD was not detected in Hp1-expressing neurons. (*b*) Average AMPA-EPSCs at −60 mV recorded before and 30–35 min after LTD induction. (Scale bars: 20 pA and 20 ms.) (*c*) Summary of changes after LTD: In control neurons, EPSCs decreased to 0.51 ± 0.08 of baseline ($n = 11$), significantly different from Hp1 (0.98 ± 0.18, $n = 7$, $P < 0.02$). Control pathways were stable (0.92 ± 0.16 and 0.98 ± 0.19).

weakening to occur (31). Studies in culture have linked removal of PSD-95, or signaling through PSD-95-associated complexes (32–35) to loss of AMPA-Rs, and suggested this may underlie synaptic depression. Here we tested directly whether knockdown of PSD-95 affects LTD in slice cultures. We find that pairing-induced LTD reduced AMPA-EPSCs by ~50% in control cells, but no LTD was observed in neurons from sister cultures that expressed Hp1 (Fig. 7). Regardless of the precise mechanism, our data suggest that PSD-95 is important in mediating some aspect of LTD.

Discussion

Remodeling of synapses and modification of their strength underlie activity-dependent plasticity. We addressed the function of PSD-95 in these processes using RNAi knockdown in slice cultures at a period in development when activity drives synaptic changes. With the surrounding network intact, we asked how individual neurons respond to transient loss of PSD-95. We show that appropriate levels of PSD-95 are required for regulation of synaptic strength and functional maturation of synapses that is normally driven by spontaneous activity. Furthermore, PSD-95 participates in the accompanying structural changes in spine density and morphology. After LTP, synaptic transmission can be transiently potentiated, but spine restructuring and stabilization are impaired when PSD-95 is knocked down. Last, appropriate levels of PSD-95 appear critical for LTD to occur.

In contrast to previous work showing specific regulation of AMPA-mediated EPSCs by PSD-95 (36, 37), we find that NMDA-EPSCs are also moderately reduced. Factors such as onset, length, and efficacy of altering PSD-95, as well as the number of manipulated neurons in the network, may affect outcome. Failure to acquire or stabilize AMPA-Rs could ultimately lead to synaptic loss. Because most synapses in CA1 are thought to contain NMDA-Rs (38, 39), an initial decrease in AMPA-Rs could cause subsequent reduction in NMDA-Rs. Consistent with this, coregulation of AMPA-EPSCs and NMDA-EPSCs has been reported (17, 18). Knockdown of PSD-95 could also attenuate generation of new silent synapses. If formation of silent synapses does not require NMDA-R activation, this may explain why APV treatment did not occlude the decrease of NMDA-EPSCs in knockdown neurons.

All synaptic features investigated differed in knockdown neurons and age-matched controls but precisely mimicked those of younger neurons at onset of knockdown. One interpretation is that loss of PSD-95 arrests synaptic development, and appropriate levels of PSD-95 are required for maturation, and for plastic changes to proceed. Consistent with this idea, PSD-95 levels and synaptic localization increase during development, in response to activity, or after learning (11, 40, 41), and multiple mechanisms for activity-dependent transcription and translation were identified (42–44). After blocking spontaneous activity for 2–3 days [which prevents increases in AMPA-containing synapses (17, 19)], we no longer detect an effect of knockdown in paired recordings, which we interpret as occlusion. A similar protocol of activity blockade resulted in decreased synaptic PSD-95 without affecting turnover, whereas other MAGUKs were not regulated or were differently regulated (41). This suggests that over the course of days, activity may control relative abundance of PSD-95 at a population of synapses and their maturation, whereas knockdown of PSD-95 and activity blockade would block maturation in a similar way.

Although turnover of PSD-95 at synapses is thought to be slow (24–36 h) (32, 41), we found a significant reduction of PSD-95 levels at spines within 2–3 days. At least some of these spines harbor synapses with normal AMPA-R content (mEPSC size is not altered), suggesting that other mechanisms or MAGUKs participate in maintenance of theses synapses and receptors. If hippocampal synapses are challenged in mutant mice (12, 45) or by molecular replacement in cultures (37), MAGUKs can compensate for each other in maintaining transmission. Only a combination of knockout/knockdown strategies can elucidate the role for each individual MAGUK.

Overall, our findings are complementary to overexpression studies (6–9) and show bidirectional modification of synaptic transmission and spine morphology by transient changes in PSD-95. They suggest that the prime mechanism for regulating synaptic strength is PSD-95's ability to control the number of synapses expressing functional AMPA-Rs. Two manipulations that interfere with endogenous PSD-95 either by knockdown in slice cultures (this study) or expression of dominant negative PSD-95 *in vivo* (9) consistently prevented activity-driven changes in synaptic strength over the course of days. However, they had different effects on pairing-induced LTP in slice cultures: Whereas knockdown did not alter LTP 30 min after induction, expression of dn PSD-95 impaired LTP at this timescale. It is possible that knockdown (several days) and expression of dn PSD-95 (12–24 h) affect induction differently. First, signaling at smaller spines (knockdown) could be altered by spine geometry affecting calcium dynamics (46) to enable mechanisms that rescue induction. Another explanation is that PSD-95 may be normally recruited during induction and this is important for subsequent stabilization of synaptic changes, but not for initial potentiation. Because dn PSD-95 could be recruited during induction, its abnormal structure would also lead to disruption of initial potentiation. In the case of knockdown, absence of PSD-95 would not affect initial potentiation but would affect only subsequent stabilization of synaptic weight changes. In this model, increases in PSD-95 levels at spines after overexpression would bypass its recruitment during induction and result in stable potentiation, which occludes subsequent LTP.

Increased strength is accompanied by structural changes after LTP (21), and structural remodeling is proposed to lock in initial synaptic weight changes on the timescale of hours and days (31). Consistent with this model, compromised structural changes and spine stabilization during knockdown could lead to the observed failure to stabilize increases in synaptic strength over several days. It also suggests that PSD-95 signaling or availability at synapses may serve as one link between early and long lasting, stable changes at synapses. In contrast to overexpression, where LTD was enhanced, (7, 8), decreasing PSD-95 levels resulted in the absence (or severe reduction) of LTD, suggesting PSD-95 content at synapses may be one of the factors determining their ability to undergo LTD. We cannot discriminate whether this is attributable to block or occlusion, but both scenarios are consistent with PSD-95 mediating some aspect of LTD.

In conclusion, our study using a knockdown approach indicates that PSD-95 is critical for several aspects of activity-dependent structural and functional plasticity. Because PSD-95 is a multidomain molecule, further work, e.g., using molecular

replacement strategies with mutant forms of PSD-95, may reveal how different domains and interactions participate in different aspects of PSD-95 function.

Methods

Constructs and Expression. Two sequences from rat PSD-95 mRNA (GenBank accession no. M96853) were targeted with shRNAs: Hp1, AATACCGCTACCAAGATGAAGACACG-CCC; Hp2, ACATCTGGGTCCCAGCCCGAGAGAGACTC. Constructs with the human RNA polymerase III promoter driving hairpin expression were generated by PCR with pGEMSP6-Zeo-U6 (provided by G. Hannon, Cold Spring Harbor Laboratory, Cold Spring Harbor, NY) as template and cloned into pBluescript (Stratagene, La Jolla, CA) . The control shRNA (Scr1) targeted AGAACACACGCAATCGAGCAC-CCTAGATC, a sequence not present in known rat genes or ESTs. We coexpressed shRNAs with GFP (pEGFP-C1; Clontech, Mountain View, CA) at a 3:1 ratio by biolistic gene transfer. Expression was 2–3 days in all experiments, except for SI Fig. 13.

Slice Cultures and Pharmacological Treatments. Hippocampal slice cultures were prepared from postnatal day 6–7 rats as described (9) and maintained for ≈1 week before transfection unless otherwise stated. In some experiments, activity was blocked by adding 10 mM $MgCl_2$ (Sigma, St. Louis, MO), 1 μM TTX (Calbiochem, San Diego, CA), or 100 μM D,L-APV (Sigma) to the culture medium at transfection.

Electrophysiology. Whole-cell recordings were obtained simultaneously from neighboring control and transfected CA1 neurons, and EPSCs were evoked, acquired, and analyzed as described (9). LTP was induced by pairing 3-Hz stimulation with postsynaptic depolarization to 0 mV for 180 seconds, and LTD was induced by pairing 1-Hz stimulation with postsynaptic depolarization to −40 mV for 500 pulses. AMPA-mEPSCs were recorded at −60 mV in 100 μM APV and analyzed as described (9). Data are shown as mean ± SEM; n is the number of cells or cell pairs. For paired data we used Wilcoxon tests, and in other cases we used unpaired Student's t tests.

Two-Photon Laser-Scanning Microscopy and Image Analysis. Images were collected on a custom-built two-photon microscope based on the Fluoview system (Olympus, Center Valley, PA). The light source was a mode-locked Ti:Sapphire laser (Chameleon; Coherent, Santa Clara, CA) tuned to 910 nm. The microscope was equipped with a ×60, 0.9 N.A. water immersion lens. Images were acquired in z-steps of 0.5 μm and analyzed offline by using software written in MatLab (MathWorks, Natick, MA). Background-subtracted integrated fluorescence was taken as a measure for spine volume after normalizing to mean fluorescence at soma and large apical dendrite (22, 28). Spine types were scored blindly. Experiments for shRNA and controls were conducted on sister cultures.

Time-Lapse Imaging and Chemical LTP. For turnover experiments, dendrites were imaged every 30 min at 30°C. In cLTP experiments, dendrites were imaged for a 30-min baseline period, and global changes were induced and measured as previously described (22, 27). The age of cultures was 14 Div plus 3 days expression, as the cLTP protocol was established for these conditions. Changes in spine size and turnover were monitored for 2 h after cLTP. Spine TOR was calculated as spines added and lost between images and per micrometer of dendrite.

We thank G. Hannon for cDNA, N. Dawkins for technical assistance, S. Newey and D. Tervo for help with dissociated cultures, and C. Kopec and M. Reigl for programming. We thank S. Kuhlman and K. Zito for comments on an earlier version of the manuscript and members of the R.M. laboratory for discussions. This work was supported by the National Institutes of Health and the Alle Davis and Maxine Harrison Endowment (R.M.).

1. Scannevin RH, Huganir RL (2000) *Nat Rev Neurosci* 1:133–141.
2. Malinow R, Malenka RC (2002) *Annu Rev Neurosci* 25:103–126.
3. Bredt DS, Nicoll RA (2003) *Neuron* 40:361–379.
4. Collingridge GL, Isaac JT, Wang YT (2004) *Nat Rev Neurosci* 5:952–962.
5. El-Husseini AE, Schnell E, Chetkovich DM, Nicoll RA, Bredt DS (2000) *Science* 290:1364–1368.
6. Schnell E, Sizemore M, Karimzadegan S, Chen L, Bredt DS, Nicoll RA (2002) *Proc Natl Acad Sci USA* 99:13902–13907.
7. Beique J-C, Andrade R (2003) *J Physiol (London)* 546:859–867.
8. Stein V, House DR, Bredt DS, Nicoll RA (2003) *J Neurosci* 23:5503–5506.
9. Ehrlich I, Malinow R (2004) *J Neurosci* 24:916–927.
10. Kim E, Sheng M (2004) *Nat Rev Neurosci* 5:771–781.
11. Sans N, Petralia RS, Wang YX, Blahos J, Hell JW, Wenthold RJ (2000) *J Neurosci* 20:1260–1271.
12. Migaud M, Charlesworth P, Dempster M, Webster LC, Watabe AM, Makhinson M, He Y, Ramsay MF, Morris RG, Morrison JH, *et al.* (1998) *Nature* 396:433–439.
13. Alvarez VA, Ridenour DA, Sabatini BL (2006) *J Neurosci* 26:7820–7825.
14. Vo N, Klein ME, Varlamova O, Keller DM, Yamamoto T, Goodman RH, Impey S (2005) *Proc Natl Acad Sci USA* 102:16426–16431.
15. Hsia AY, Malenka RC, Nicoll RA (1998) *J Neurophysiol* 79:2013–2024.
16. De Simoni A, Griesinger CB, Edwards FA (2003) *J Physiol* (*London*) 550:135–147.
17. Zhu JJ, Malinow R (2002) *Nat Neurosci* 5:513–514.
18. Groc L, Gustafsson B, Hanse E (2003) *Neuroscience* 121:65–72.
19. Barria A, Malinow R (2005) *Neuron* 48:289–301.
20. Petralia RS, Esteban JA, Wang YX, Partridge JG, Zhao HM, Wenthold RJ, Malinow R (1999) *Nat Neurosci* 2:31–36.
21. Matsuzaki M, Honkura N, Ellis-Davies GC, Kasai H (2004) *Nature* 429:761–766.
22. Kopec CD, Li B, Wei W, Boehm J, Malinow R (2006) *J Neurosci* 26:2000–2009.
23. Hering H, Sheng M (2001) *Nat Rev Neurosci* 2:880–888.
24. Esteban JA, Shi SH, Wilson C, Nuriya M, Huganir RL, Malinow R (2003) *Nat Neurosci* 6:136–143.
25. Zhu JJ, Esteban JA, Hayashi Y, Malinow R (2000) *Nat Neurosci* 3:1098–1106.
26. Yasuda H, Barth AL, Stellwagen D, Malenka RC (2003) *Nat Neurosci* 6:15–16.
27. Otmakhov N, Khibnik L, Otmakhova N, Carpenter S, Riahi S, Asrican B, Lisman J (2004) *J Neurophysiol* 91:1955–1962.
28. Holtmaat AJ, Trachtenberg JT, Wilbrecht L, Shepherd GM, Zhang X, Knott GW, Svoboda K (2005) *Neuron* 45:279–291.
29. Marrs GS, Green SH, Dailey ME (2001) *Nat Neurosci* 4:1006–1013.
30. Prange O, Murphy TH (2001) *J Neurosci* 21:9325–9333.
31. Malenka RC, Bear MF (2004) *Neuron* 44:5–21.
32. El-Husseini AE, Schnell E, Dakoji S, Sweeney N, Zhou Q, Prange O, Gauthier-Campbell C, Aguilera-Moreno A, Nicoll RA, Bredt DS (2002) *Cell* 108:849–863.
33. Colledge M, Snyder EM, Crozier RA, Soderling JA, Jin Y, Langeberg LK, Lu H, Bear MF, Scott JD (2003) *Neuron* 40:595–607.
34. Kim MJ, Dunah AW, Wang YT, Sheng M (2005) *Neuron* 46:745–760.
35. Dell'acqua ML, Smith KE, Gorski JA, Horne EA, Gibson ES, Gomez LL (2006) *Eur J Cell Biol* 85:627–633.
36. Nakagawa T, Futai K, Lashuel HA, Lo I, Okamoto K, Walz T, Hayashi Y, Sheng M (2004) *Neuron* 44:453–467.
37. Schluter OM, Xu W, Malenka RC (2006) *Neuron* 51:99–111.
38. Isaac JT, Nicoll RA, Malenka RC (1995) *Neuron* 15:427–434.
39. Liao D, Hessler NA, Malinow R (1995) *Nature* 375:400–404.
40. Skibinska A, Lech M, Kossut M (2001) *NeuroReport* 12:2907–2910.
41. Ehlers MD (2003) *Nat Neurosci* 6:231–242.
42. Bao J, Lin H, Ouyang Y, Lei D, Osman A, Kim TW, Mei L, Dai P, Ohlemiller KK, Ambron RT (2004) *Nat Neurosci* 7:1250–1258.
43. Akama KT, McEwen BS (2003) *J Neurosci* 23:2333–2339.
44. Todd PK, Mack KJ, Malter JS (2003) *Proc Natl Acad Sci USA* 100:14374–14378.
45. Klocker N, Bunn RC, Schnell E, Caruana G, Bernstein A, Nicoll RA, Bredt DS (2002) *Eur J Neurosci* 16:1517–1522.
46. Oertner TG, Matus A (2005) *Cell Calcium* 37:477–482.